ADVANCED FUNCTIONAL MATERIALS
www.afm-journal.de

Photoinduced Colossal Magnetoresistance under Substantially Reduced Magnetic Field

Tomi Elovaara, Sayani Majumdar, Hannu Huhtinen, and Petriina Paturi*

The colossal magnetoresistive insulator to metal switching of almost nine orders of magnitude under the significantly reduced magnetic field is achieved by illumination for the low bandwidth manganite thin films. Similarly, by changing the measuring bias voltage through the sample the required magnetic field for insulator–metal transition can be further fine-tuned. By applying a magnetic field of suitable strength, the samples can also be tuned to be extra sensitive to the illumination having colossal effect on the resistivity at low temperatures. This kind of utilizing of multiple external stimulants, which together change the properties of the material, could have significant impact on the new generation of phase-change memories working under affordable conditions.

1. Introduction

Insulator-to-metal transition (IMT) phenomena in complex oxides are a topic of great scientific and technological interest due to their potential applications in resistive memories.[1–7] In transition metal oxides, the nonvolatile insulator to metal resistive switching is achieved when the strongly correlated electrons of the initial Mott insulator state are released to the conduction band by external stimuli, such as electric field, magnetic field, pressure, or illumination. These phase transitions are quite complex and show interplay of charge, spin, orbital, and crystal orderings, not yet completely clarified and hence explored. For technological applications, it is also important to study how efficiently these transitions can be driven from one phase to another. The small-bandwidth manganite $Pr_{1-x}Ca_xMnO_3$ (PCMO), with x = 0.3–0.5, is known for colossal magnetoresistance (CMR), where the drastic reduction of electrical resistance is achieved by applying a sizable electric or magnetic field which melts the insulating charge ordered (CO) phase.[8,9] This IMT in PCMO is also related to the metamagnetic first-order phase transition from antiferromagnetic (AFM) to ferromagnetic (FM) phase.[10]

The CMR effect is huge for PCMO compounds where the CO phase is established, but the IMT transition demands a very high magnetic[9,11] or electric [8] field which is not suitable for technological applications. Recently we reported that metamagnetic transition can be achieved in a relatively low magnetic field for structurally improved PCMO (x = 0.4 and 0.5) thin films compared to the bulk samples.[12] Photoinduced melting of CO phase was previously demonstrated by Miyano et al.[13] and Takubo et al.[14,15] where an IMT was obtained under a strong electric field. Recent report of Beaud et al. showed an ultrafast photoinduced breaking of CO phase at 100 °C temperature in PCMO x = 0.5 thin film.[16] We have earlier observed an increase in FM phase at the cost of AFM phase under illumination at the low temperature coexisting FM–AFM phase of low-hole doped PCMO (x = 0.1) thin films[17] which could be related to IMT transition in this strongly correlated system. In this paper, we report that by illumination CMR of almost nine orders of magnitude can be achieved in PCMO (x = 0.4) thin film under 50% less applied magnetic field compared to that in dark. We term this combined effect of light and magnetic field on the sample resistance as magnetophotoresistance (MPR). Also by changing the measuring bias voltage, the required magnetic field can be fine-tuned. The result could have significant impact on the new generation of phase-change memories working under affordable conditions.

2. Results

The PCMO thin film samples for this study were selected to have considerably strong CO phase with metamagnetic AFM to FM transition. The two films were chosen based on their sizable difference in magnetic field required for AFM to FM transition, for a better insight of the illumination effects on different strengths of CO phases (see the Supporting Information). The sample with the weaker CO phase is PCMO x = 0.4 with in situ annealing treatment at 500 °C, called p40–500. The stronger CO phase is on the PCMO x = 0.5 sample with in situ annealing treatment at 700 °C, called p50–700. More detailed information of the samples is given in the Experimental Section.

The magnetoresistive measurements were executed with a standard two-point connection in Quantum Design physical property measurement system (PPMS) with fiberoptic

T. Elovaara, Dr. S. Majumdar, Dr. H. Huhtinen, Prof. P. Paturi
Wihuri Physical Laboratory
Department of Physics and Astronomy
University of Turku
FI-20014 Turku, Finland
E-mail: tomi.elovaara@utu.fi
Dr. S. Majumdar
Nanomagnetism and Spintronics Group
Department of Applied Physics
Aalto University School of Science, P.O. Box 15100
FI-00076 Aalto, Finland

DOI: 10.1002/adfm.201502233

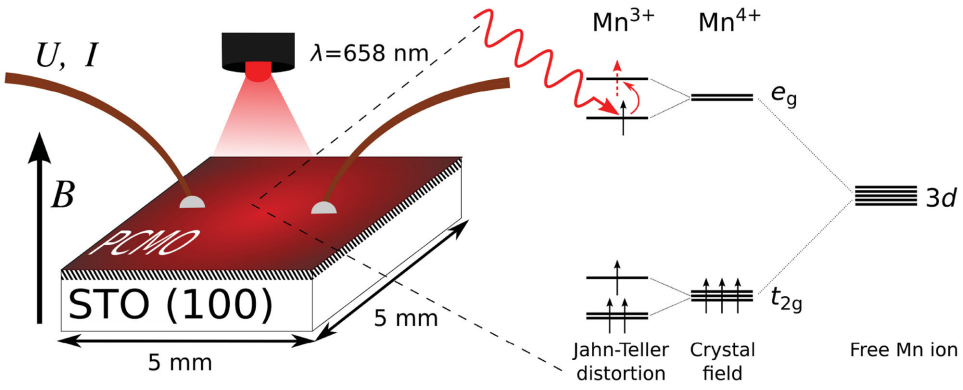

Figure 1. Schematics of the measurement setup (left) and the intrasite photo excitation of Mn^{3+} ion's electron (right). The Mn 3*d* band is split into t_{2g} and e_g due to the cubic crystal field. These bands are further split due to distortions of oxygen octahedra (Jahn–Teller effect), at the Mn^{3+} sites.

(1.88 eV, with 55–400 μW mm^{-2} fluence) sample holder connected to a Keithley picoammeter. A schematic of the magnetoresistive measurement setup is presented in **Figure 1**. More detailed information about the measurements is given in the Experimental Section.

2.1. Magnetoresistive Virgin Measurement

In the performed magnetoresistive measurements, the illumination generally lowers the resistivity of the films. At room temperature, the effect of illumination is minimal on resistivity, but starts to increase as the temperature is decreased and becomes pronounced below the Curie temperature. The highest MPR effect was obtained in the virgin measurement where the samples were first cooled without the magnetic field to 10 K and after that the background magnetic field was slowly (4 mT s^{-1}) brought up to 8 T. The measurement was made in dark and under illumination and repeated with two different voltage ranges. The virgin measurements at 10 K with high-voltage range (up to 200 V) are presented in **Figure 2** for both of the samples. The virgin measurements data with low-voltage range (up to 50 V) are shown in the Supporting Information. The effect of illumination is evidently visible on the resistivity (ρ) and IMT, as the illumination drastically reduces the required magnetic field for IMT. The transition field decreases by 50% under the illumination from 4.4 T to 2.2 T for sample p40–500 and by 27% from 7.6 T to 5.5 T for sample p50–700. The IMT field is calculated from the point where sharp drop of resistivity starts. Also, the used bias voltage has a similar influence on the IMT field as the illumination, although the effect is smaller. The higher voltage range reduces the transition field by almost 0.5 T both in dark and under illumination. Therefore by using the electric field on top of light and magnetic field, it is possible to fine-tune the IMT (see the Supporting Information). For both the samples, the IMT is generally very sharp but gets slightly broader under light and with smaller voltage range. The initial drop in resistivity during the transition is around seven orders of magnitude for both samples. After the transition, the resistivity continues to decrease as the background magnetic field increases, making the whole resistivity change even higher. This slow decrease in resistivity with the increase in magnetic field is associated with the high field MR effect in metallic phase of manganites due to increase in FM volume fraction with increasing field. The overall CMR effect at 8 T field, calculated using the formula $(R_{0T} - R_{8T})/R_{8T}$, where R_{0T} is the sample resistance at $B = 0$ and R_{8T} is the resistance at 8 T field, is $\approx 7 \times 10^8$ in dark and $\approx 1 \times 10^9$ under illumination for sample p40–500. The CMR effect is smaller for sample p50–700, where the values are $\approx 8 \times 10^6$ in dark and $\approx 5 \times 10^6$ under illumination. The smaller overall CMR effect values for sample p50–700 can be explained with higher magnetic field required for IMT

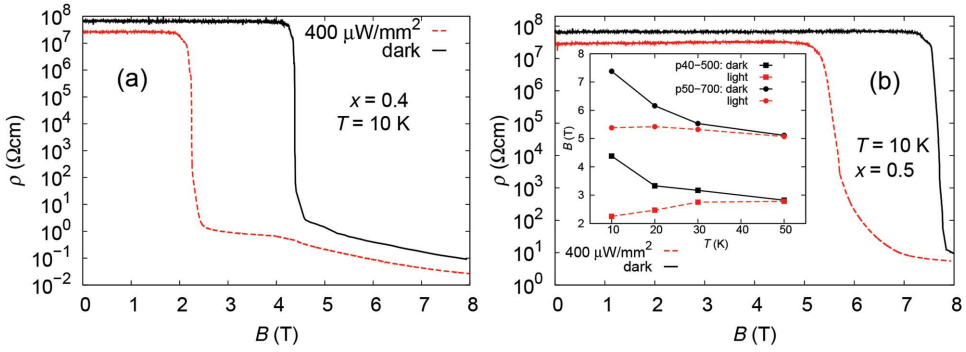

Figure 2. IMT measured at 10 K in dark (solid line) and under illumination (dashed line) while the external magnetic field is slowly risen to 8 T for the first time (virgin) for both samples a) p40–500 and b) p50–700. The inset of (b) is the temperature dependence of IMT field in dark and under illumination. The IMT field is calculated from the point where sharp drop of resistivity starts.

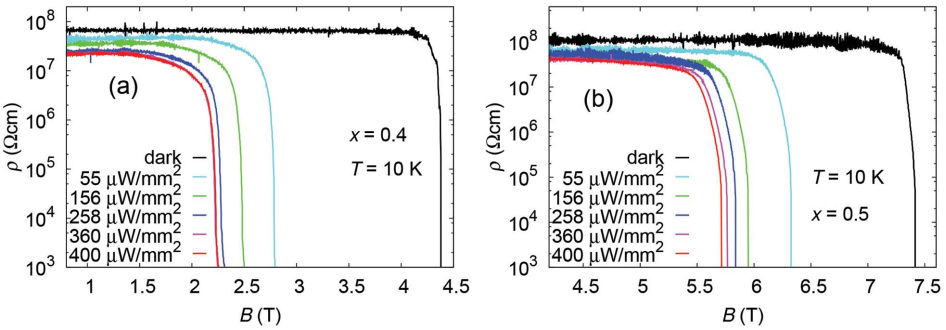

Figure 3. Magnetoresistive virgin measurement at 10 K with varying laser fluences for both samples a) p40–500 and b) p50–700.

which is very close to the maximum magnetic field used in our measurements. Similarly, IMT does not occur at all under 8 T field for sample p50–700 in dark with low voltage range (see the Supporting Information).

The magnetoresistive virgin measurements were repeated at several temperatures (10, 20, 30, 50, and 80 K; see the Supporting Information) and the corresponding IMT fields with and without illumination are presented in the inset of Figure 2b. The MPR effect on the transition field diminishes as the temperature rises, and is almost zero at 50 K. As the temperature increases, the IMT gets wider and the sharpness of IMT reduces. At 80 K, there was no effect of illumination on IMT field and, on the other hand, the CMR effect was decreased, being over 5 decades for the p40–500 sample and only 2 decades for the p50–700 sample. In dark, the transition field decreases steeply as the temperature is increased to 50 K for both samples. Under illumination, the transition field increases moderately for sample p40–500 and decreases slightly for sample p50–700 as the temperature is increased to 50 K. Also, the effect of illumination decreases when the temperature is increased and disappears completely when the temperature is higher than the Curie temperature. At first glance, it seems that the illumination and increasing the temperature has similar effects on the transition field. However, for sample p40–500 the lowest transition field is achieved by illuminating the sample at low temperature and not by heating the sample. Anyway, to conclusively prove that the observed effect is due to illumination and not due to heating, we have to exclude the effect of laser-induced heating of the sample. To do this we made the field cooled resistivity measurements under magnetic field where the sample is in the metallic phase. In these measurements at the low-temperature regime under magnetic field the resistivity of both samples decreases with lowering of temperature and the effect of illumination reduces the resistivity even more (see the Supporting Information, Figure S5). However, as the resistivity is directly commensurate to temperature at low temperatures under magnetic field, the possible heating effect of illumination should increase the resistivity but not the other way around. Detailed discussion of possibility of sample heating is presented in the Supporting Information to show that this photoinduced change in IMT is indeed due to photoillumination and not a result of laser-induced heating of the sample.

To further study the influence of illumination on the IMT field the magnetoresistive virgin measurements at 10 K were repeated with several laser fluences (55, 156, 258, 360, and 400 μW mm^{-2}). As can be seen from **Figure 3**, even the lowest laser fluences bring about an immense reduction to the IMT field for both samples. The MPR of both the samples is similar in a way that the IMT field decreases as the laser fluences are increased. The change is very prominent at lower fluences but then slows down as the fluences increase. For sample p40–500, the change in IMT field even saturates at high laser fluences, as the IMT field is exactly same for fluences of 360 and 400 μW mm^{-2}.

2.2. Magnetoresistive Loop Measurements

The magnetoresistive loop measurements $\rho(B)$ were performed in dark and under light at 10, 20, 30, and 50 K while the magnetic field was ramped from 8 T to −8 T and back at the rate of 188 mT s^{-1}. The loop measurements were done after the virgin measurements. The loop measurements at 10 K are presented in **Figure 4** for both samples. The measurements at other temperatures are presented in the Supporting Information, Figure S4. The change in resistivity in the loop measurements at 10 K is much smaller in comparison with the virgin measurements and the maximum resistivity is only a fraction of the initial resistivity in the virgin measurements. This means that at 10 K temperature, once the CO phase is melted under high magnetic field, both of the samples stay in the metallic phase and do not return to the insulating phase as the magnetic field returns to zero. However, the loop measurements at 50 K show a colossal change in resistivity in both of the samples together with a large hysteresis effect, while the effect of illumination stays low. These observations, where the loop hysteresis in high field range increases with increasing temperature, are in line with the magnetic loop measurements of similar films.[12] This indicates that the observed metastable metallic phase might have close correlation to the related metamagnetic AFM to FM transition phenomena, where the bulk samples of the same materials are locked in the metastable FM phase and do not return to the AFM phase until the temperature is high enough to induce enough thermal activation energy to overcome the spin localization.[10] In this metastable FM-metallic phase, when the magnetic field is turned back to zero, illumination seems to push the samples to a comparatively higher resistance state, as can be seen in Figure 4. The low resistance metallic phase is more persistent in sample p40–500 than in sample p50–700 in the applied magnetic field range. The reason for this is probably

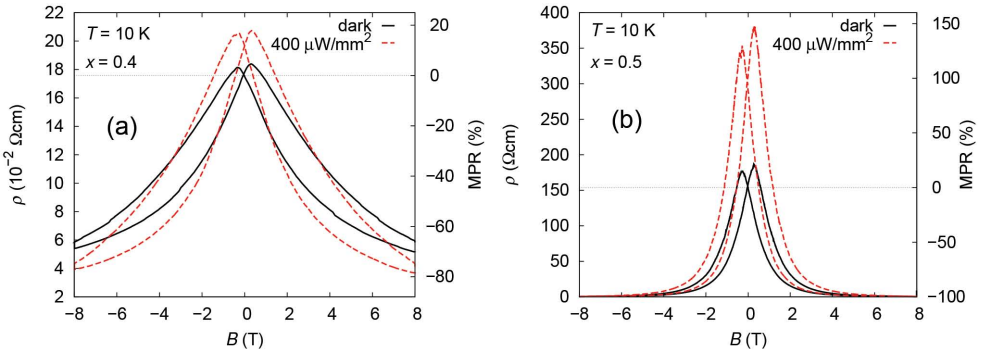

Figure 4. Magnetoresistive loops at 10 K measured in dark (solid black) and under illumination (dashed red) for both samples a) p40–500 and b) p50–700 with calculated magnetophotoresistance (MPR) percentage $[(R_H - R_{0T\text{-}dark})/R_{0T\text{-}dark}]\cdot 100\%$.

that applied 8 T magnetic field is barely enough to induce the IMT in sample p50–700, whereas it is well beyond the required field for IMT in sample p40–500. Therefore, the used 8 T is not sufficient to completely lock the metallic phase in sample p50–700. This also indicates that by controlling the magnetic field, we can adjust the stability of the metastable metallic phase. It is interesting, how the illumination lowers the IMT field, but at the same time the illuminated metallic phase is less persistent when the magnetic field is withdrawn. To clarify this better, we measured the temporal resistivity response to illumination under various conditions for both the samples.

2.3. Temporal Resistivity Measurements

The first case of the temporal resistivity measurements is made at the insulating phase of the samples without a magnetic field and hence, the effect is termed photoresistance (PR). These PR measurements were done with different laser fluences and the dynamical response to illumination was measured as a function of time at 10 K. As can be seen from **Figure 5**, the illumination reduces the resistivity and the effect is strongly dependent on laser fluence. The resistivity drop is larger for higher laser fluences with maximum of almost 60% for p40–500 and 80% for p50–700. However, the illumination does not induce IMT, as the maximum resistivity drop is less than a decade. The resistivity response to the illumination starts or ends in less than a second while turning the laser on or off for both samples at higher fluences, indicating normal semiconductor like transient photoconductivity where the illumination excites the carriers across the bandgap and increases the free electron and electron hole concentration.[18]

In the second case we measured the temporal response of the resistivity to the illumination at 10 K with two different fluences (156 and 400 μW mm^{-2}) in the metallic phase, i.e., in the presence of a background magnetic field, we noticed different resistive response from the samples compared to the insulating phase (see the Supporting Information, Figure S6). In the metallic phase under a magnetic field the illumination reduced the resistivity but the resistivity did not return to its initial value when illumination was switched off. Therefore, in the metallic phase under magnetic field we could reduce the resistivity as a function of exposure time of light. However, the effect of light reduced as the resistivity decreased. This effect was achieved with both of the used laser fluences. Similar effect is reported for $Pr_{0.5}Ca_{0.5}MnO_3$ thin films under X-ray radiation without magnetic field where the persistent resistivity switch as a function of exposure time was achieved by Garganourakis et al.[19] The effect was explained with photodoping where exposure to high energy X-rays (642.5 eV) created defects in the CO/OO phase and the destruction of CO/OO phase creates deep donor level impurities. These impurities got ionized and the corresponding electrons were excited to the conduction band, lowering the resistivity and effectively mimicking the lowering of the Ca concentration. The authors also show exposure time and X-ray intensity dependence of the effect. In the present measurements, although similarities like

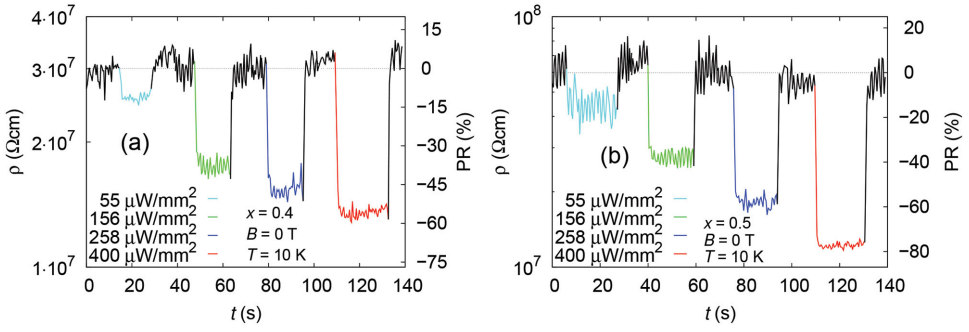

Figure 5. The temporal resistivity response to illumination measured at 10 K with laser fluences of 55, 156, 258, and 400 μW mm^{-2} and without magnetic field for both samples a) p40–500 and b) p50–700 with calculated photoresistance (PR) percentage $[(R_{ill.} - R_{dark})/R_{dark}]\cdot 100\%$. The black color indicates the sample without illumination.

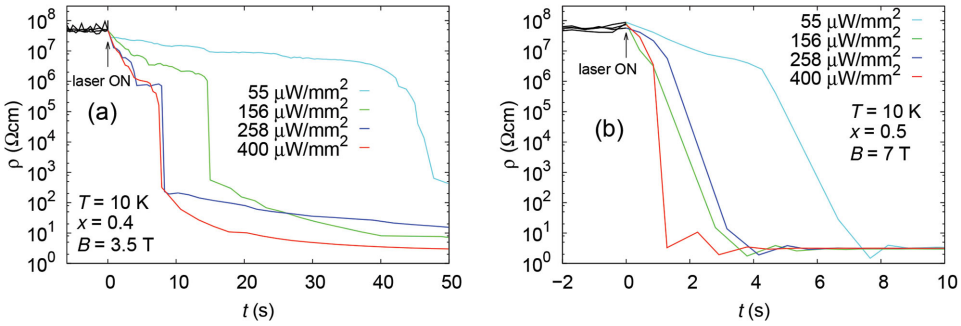

Figure 6. The temporal resistivity response to illumination measured for the samples a) p40–500 and b) p50–700 under 3.5 and 7 T (respectively) background magnetic field at 10 K with laser fluences of 55, 156, 258, and 400 μW mm^{-2}. The black color indicates the sample without illumination.

fluence dependence exist, strong differences can be observed. In MPR effect, the system is driven from insulator to metal phase showing orders of magnitude change in resistivity. Also, at the insulating phase (i.e., in the absence of a magnetic field), resistance showed fast response to illumination, whereas IMT and resistivity at metallic phase showed slower time dependence. After removing light, another distinctive feature is the resistance returning to original value in the insulating phase in the absence of magnetic field, whereas the resistance is permanently changed due to photodoping. This might have its origin in the fact that instead of high energy X-ray radiation the magnetic field is used to melt the CO/OO phase in our measurements at low temperatures inducing a phase transition and creation of trapped deep donor level impurities. These defects induce a local deformation to the crystal lattice due to the strong coupling between electrons and lattice. As the low energy illumination excites an electron to the conduction band from the impurity, it relaxes the local lattice deformation around the defect and hence, the exited electron stays in the conduction band making the reduction of resistivity persistent. The effect of illumination is again higher for sample p50–700 which can be explained with higher magnetic field required for the phase transition and, hence, the high field MR effect in metallic phase is smaller compared to sample p40–700. Therefore, it is easier to give extra push to the phase transition toward metallic phase with the illumination to sample p50–700 under 9 T applied magnetic field.

The third case of temporal measurements was measured at 10 K with two different fluences (156 and 400 μW mm^{-2}) in the metallic phase without magnetic field. This was achieved by applying 9 T magnetic field and then reducing the field back to zero, thus the sample stayed in the metallic phase, as observed in the above loop measurements. In the metallic phase with zero magnetic field, the sample resistivity increased under illumination with both fluences and did not return to its initial value when illumination was switched off (see the Supporting Information, Figure S7). This effect is consistent with the loop measurement data in Figure 4 around zero magnetic field. Also, the effect of illumination decreased as the resistivity got higher. The overall effect is larger for sample p50–700, which is in good agreement with the loop measurements. It seems that the illumination helps the sample to return from the metastable metallic phase toward a more resistive state. This has been discussed later in detail.

2.4. Magnetic Biasing

The observed effects can be unified in one single measurement which is presented in **Figure 6**. This was done by optimizing the magnetic field to maximize the light-induced effect. The background magnetic field was selected so that it lies between the IMT fields measured in dark and under illumination, i.e., 3.5 T for sample p40–500 and 7 T for sample p50–700. By utilizing this magnetic biasing of the sample, we could induce the IMT by using only illumination, as can be seen from Figure 6. Compared to the photoresponse without magnetic field at 10 K, the time for completion of IMT process is slower. Also the IMT takes much longer for sample p40–500 than for sample p50–700 and the level of resistivity varies with different laser fluences at metallic phase for sample p40–500. These differences between the samples are caused by the applied magnetic field of 7 T, which is closer to the IMT transition field value in dark for sample p50–700, whereas the applied magnetic field of 3.5 T is rather small compared to 4.4 T needed for IMT at dark for p40–500 and so the IMT is not so intense for sample p40–500. Furthermore, the speed of the IMT could be fine-tuned with the used laser fluence. With lower fluence the IMT progress is slower. This indicates that changes in resistance can be induced instantly with photoexcitation but to form a metallic conductive channel, either a strong fluence or a longer exposure is needed. Resistivity at metallic phase could be fine-tuned by changing the illumination exposure time if the illumination was turned off during the IMT until the lowest resistivity value was reached. So we could dynamically induce the IMT by illumination and fine-tune the intensity of transition with background magnetic field, illumination fluence, and exposure time. To explain the observed effect, we have to take a closer look at the nanoscale phase separation picture in the manganites, which will be discussed in detail later in the article.

3. Discussion

In order to fully exploit the photoinduced reduction of melting field for CO phase, we need to get deeper insight of the complex electron correlation and coexisting multiple phases in manganites. In the perovskite manganites, the degenerate Mn 3*d* electronic states are split into the threefold t_{2g} and twofold e_g levels due to a cubic crystal field effect rising from hybridization and

electrostatic interaction with surrounding oxygen octahedra. In the Mn^{3+} sites, the degeneracy of e_g levels is further split as the occupied e_g orbital hybridizes with the adjacent oxygen $2p$ orbital lowering the overall energy. The scheme of this Mn $3d$ band splitting is presented in Figure 1. The optimal hybridization depends on the symmetry of the surrounding electron orbitals and hence the minimization of energy induces local distortions in $Mn^{3+}O_6$ octahedra where some of the Mn—O bonds get shorter and other longer, i.e., causing the Jahn–Teller distortion.[20] This is why the e_g electrons interact with the distortions of the surrounding lattice, i.e., phonons. Phonons are strongly coupled with surrounding oxygen octahedra. This kind of dynamic electron–phonon interaction leads to the formation of polarons. In the formation stage of the CO/OO phase, the charge and elongated Mn^{3+} $3d$ orbitals order themselves leading to the change of lattice symmetry from orthorhombic *Pbnm* to monoclinic $P2_1/m$.[16,21] This is the so called site-centered CO model, where the octahedron around Mn^{3+} is distorted and the octahedron around Mn^{4+} is rather regular.[21–23] In addition, another CO model exists, where the charge is localized not on sites but on bonds.[24,25] In the bond-centered CO phase, the valences of the Mn ions are $Mn^{+3.5+\delta}$/$Mn^{+3.5-\delta}$ and all the octahedra are elongated similarly so that two octahedra connect along their elongated direction forming a Mn–Mn dimer (Zener polaron).[24] There have also been calculations where these two CO models could coexist leading to a noncentrosymmetric lattice distortion and thus a ferroelectric state.[26–28] Albeit the detailed microscopic structure of this CO phase remains to be elusive, it is clear that CO phase couples strongly to the lattice via the orbital degree of freedom.[29]

In PCMO, CMR arises when the application of a large magnetic field destroys the insulating CO/OO phase as the high magnetic field tends to align the local spins of Mn ions ferromagnetically. The magnetic field induces torque to the spins and increases the Mn—O—Mn bond angles toward 180°, affecting the Mn—O bond lengths and modifying the overlapping of hybridized orbitals.[10,30] The outcome of this is increasing electron hopping amplitude and broadening of the bandwidth W of the e_g-band, which together mobilize the e_g electrons, give rise to the FM metallic phase. During the process, the modified MnO_6 octahedra induce the structural first-order phase transition as the background magnetic field lifts the system from the energy minimum to the metastable phase. The transition back from the metastable to the stable phase occurs by overcoming a free-energy barrier.[31] Hence, the CO/OO ordering is not alone sufficient to enable the CMR phenomenon, but also the AFM ordering has to be formed in order to activate the spin degree of freedom which can be influenced by magnetic field. In addition, the CMR effect is visible below the Néel temperature T_N and gets more intense when temperature decreases, aligning more spins and forming increasing amount of FM clusters in the AFM matrix forming frustrated magnetic phase.

Under the illuminating laser, the PCMO samples are exposed to photons with 1.88 eV energy with 55–400 μW mm^{-2} fluence which mainly excite the Mn^{3+} intrasite transition ($e_g^1 \rightarrow e_g^2$; see Figure 1),[32] and which, in turn, drive the relaxation of the Jahn–Teller distortion.[16,33,34] As the e_g electron changes its orbital during the excitation, the orbital symmetry changes resulting in a destabilization of the Jahn–Teller distortions of surrounding MnO_6 octahedron. According to Beaud et al.,[16] the optical stimulus also melts the charge and orbital ordering and simultaneously excites the optical phonon modes. Basically, the illumination excites a polaron which causes a high energy lattice vibration, i.e., optical phonon to the sample. This photoinduced vibration of the crystal lattice in PCMO thus leads to a new equilibrium state with modified charge distribution. This greatly decreases the required magnetic field for IMT, as the CO/OO phase is already destabilized and the atoms vibrate more. Similar decrease in the transition field is also achieved with rising temperature, where the lower energy phonons/vibrations are created due to sample heating. The photoexcited phonons also enhance the sample resistance at metallic phase in the absence of magnetic field, i.e., when Mn spins are not aligned, as observed in Figure 4 and Figures S4 and S7 (Supporting Information). Enhanced resistance in metallic phase under illumination without a magnetic field can be the result of increased scattering of optical phonons and conduction electrons by the magnons. In the FM phase of perovskites, electron–magnon scattering is an important phenomenon controlling the conductivity and it was shown before that under a magnetic field, electro–magnon scattering is suppressed due to ordering of magnons.[35] In the present case, in the absence of a magnetic field increased electron–magnon and electron–phonon scattering[36] can turn the system to a higher resistance state. Also, similar effect was previously reported by Takubo et al.[15] where a persistent photoinduced reverse IMT process, i.e., metal–insulator transition, was confirmed for manganite thin film. The effect was explained with 2.3 eV photons that could spin-flip the e_g electrons against the Hund-coupling energy and induce the transformation from FM metallic (FMM) to CO insulating phase. However, in our case the effect of light is much more prominent in turning the sample into the metallic phase than out of it, as the optical stimulus of used laser alone is not strong enough to overcome the free-energy barrier of the metastable metallic phase.

The used maximum voltage in the measurements changes the electric field through the sample which also affects the IMT field, lowering it around 0.5 T at 10 K with the increased electric field. This indicates that at the coexisting AFM-FM phase, when small FMM clusters start to form inside the material, the applied electric field can induce tunneling of electrons between FMM domains separated by the insulating AFM domain boundaries. This can induce some conducting channels inside the insulating background in the sample causing an IMT. In this case, it is important to remember that the conduction of electrons can take place through a few channels only while the rest of the sample is still in the insulating phase. Under photoexcitation, when the metallic FM domains increase considerably, an applied electric field is able to establish more conducting channels between the FMM domains, decreasing the IMT field further.

In the measurements, the light-induced effects are the most prominent at temperatures below 50 K where the films have frustrated magnetic phase, i.e., when there is a difference between the field cooled and zero field cooled magnetizations (see the Supporting Information). In this temperature regime, the CMR effect is also most intense. This frustrated magnetic phase consists of a nanoscale phase separation between AFM

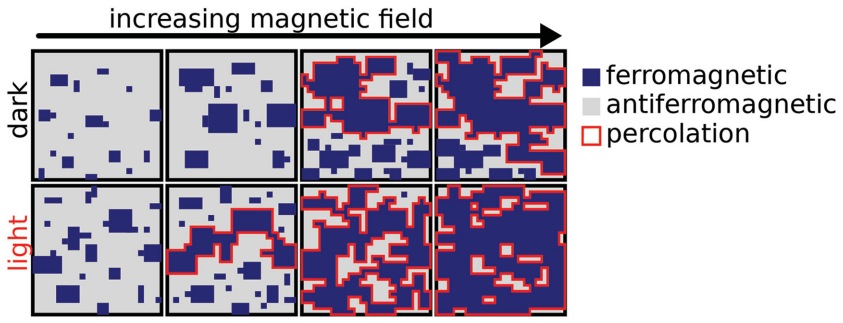

Figure 7. A schematic illustration of the nanoscale phase separation in manganites and the influence of illumination to the AFM insulating and FM metallic cluster dynamics under increasing magnetic field. The IMT occurs fast in a certain magnetic field during the magnetic field induced AFM to FM phase transition when the FM metallic clusters form a solid percolation path between the connectors. The illumination increases the efficiency of the magnetic field increasing the FM metallic clusters in the sample and hence the IMT transition occurs at reduced magnetic field.

and FM clusters, where the AFM phase is dominating,[37] as shown in **Figure 7**. The increasing background magnetic field makes the FM phase energetically more favorable and increases the FM/AFM cluster ratio in the sample. The IMT, where the FM clusters establish a solid conducting path through the sample, happens much faster than the metamagnetic AFM to FM transition. This is expected for the percolative conducting process. This is because a few conducting channels are already enough to transform the system from insulating to metal-like, whereas long-range magnetic ordering is required for AFM to FM phase transition. In addition, the resistivity continues to decrease after IMT when the magnetic field is further increased, as can be seen in Figure 2a, indicating the formation of even more FMM clusters, with increasing magnetic field. A schematic illustration of this magneto-photoinduced percolative conduction process is presented in Figure 7.

4. Conclusion

In this paper, we have shown greatly reduced magnetic field for colossal magnetoresistive Mott-transition under illumination. This achieved metallic phase is metastable and did not return back to insulating phase even when the magnetic field was turned off. The insulating phase was restored when the temperature was risen enough to overcome the free-energy phase boundary. However, the illumination of the samples by itself is unable to induce IMT for the over 100 nm thick samples and the background magnetic field is still needed to complete the IMT. By applying a steady magnetic field, we could tune the sample to be extra sensitive to the illumination having colossal effects to the resistivity at low temperature. Also with varying laser fluence and exposure time the intensity of the IMT can be influenced. Similarly, the increased electric field through the sample decreased the required magnetic field for the IMT around 0.5 T at 10 K. This indicates that combined effect of light and magnetic field induces more FMM clusters that can take part in conduction under applied electric field facilitating IMT. This combined effect of multiple external stimulants, which together change the properties of the material, improves the efficiency to drive the IMT, which can be very useful in future technological applications. It can also be emphasized that the resistive switching phenomenon in our samples is a nonvolatile process, affecting the electron states and not the ions making the samples very fast-operating and endurable for energy-efficient technological purposes.[1]

5. Experimental Section

Sample Preparation and Characterization: PCMO films were prepared by pulsed laser deposition on (100) SrTiO (STO) substrates using an excimer XeCl 308 nm laser with a pulse duration of 25 ns and a repetition rate of 5 Hz with a laser fluence of 2 J cm^{-2}. The flowing oxygen pressure in the chamber was p = 0.2 torr and the substrate temperature during the deposition was 500 °C. In order to affect the structural properties as well as the oxygen content of the films, in situ postannealing treatments were made either at 500 °C or at 700 °C in atmospheric pressure of oxygen with heating and cooling rates of 25 °C min^{-1}. Although the amount of laser pulses was same, the measured thickness of the films increases with Ca concentration, being 110 and 125 nm for films with x = 0.4 and 0.5, respectively.

The detailed structural characterization was made to the samples by X-ray diffraction analysis at room temperature using Philips X'Pert Pro diffractometer. The phase purity of the films was confirmed from the θ–2θ scans in out-of-plane (0b0) direction. Further information of the sample characteristics can be found in our previous work.[12]

Magnetoresistive Measurement: The magnetoresistive measurements were executed with a standard two-point connection in PPMS magnetometer connected to the Keithley 6487 picoammeter. The external field B was always perpendicular to the planes of the films, i.e., along the PCMO [010] axis. The copper wiring was made to the surface of film with indium brazing. The distance between the connectors was 3.5 mm. All the measurements were made in dark or under photoexcitation keeping the other experimental conditions unchanged. Photoinduced measurements were performed with a home-made fiberoptic sample holder attached to the PPMS magnetometer where the laser spot covered the whole PCMO film. The used light source was AlGaInP laser diode working at λ = 658 nm (1.88 eV) with the maximum output power of 10 mW measured at the end of the optical fiber. Hence, the total maximum output density at the sample surface was ≈0.4 mW mm^{-2}. A schematic of the measurement setup is presented in Figure 1. The fluence measurements were made by changing the laser diode current and measuring the corresponding laser output power from the end of the optical fiber with Thorlabs S120VC photodiode power sensor attached to Thorlabs power meter PM100D. The chosen fluences for the measurements were 55, 156, 258, 360, and 400 μW mm^{-2}.

During the magnetoresistivity measurements, the voltage is linearly changed so that the current stays constant at 2 μA between voltages 0.1 and 200 V. The corresponding resistivities are 0.5 Ω cm (0.1 V) and 10^3 Ω cm (200 V). In the resistivity range under 0.5 Ω cm and over 10^3 Ω cm, the measuring mode changes on the fly to the constant voltage mode where the voltage stays at 0.1 and 200 V, respectively. In the resistivity range where the constant voltage mode is used, the measuring current varies. However, the current is always kept below 2 mA at low-resistivity regions to avoid the colossal electroresistance effect.[25] The magnetoresistive virgin measurements at 10 K were repeated with two different voltage ranges: high voltage range 0.1–200 V and low voltage range 0.1–50 V. The other magnetoresistive virgin measurements were measured at constant bias voltage of 200 V. In the measurements, the electric field between connectors was 60 kV m^{-1} (200 V) and 15 kV m^{-1} (50 V). The magnetoresistive loop measurements were made

with constant voltage mode for both samples. The used voltages were 0.1 V at 10 K and 10 V at higher temperatures for sample p40–500 and 50 V at 10 K and 70 V at higher temperatures for sample p50–700. The PR measurements with different laser fluences were made with constant voltage mode at 200 V for both samples. The temporal resistivity response measurements under 3.5 and 7 T magnetic fields with different laser fluences were measured using high voltage range 0.1–200 V for both samples. The temporal measurements at metallic phase were made with constant voltage mode for both samples using 0.1 V under 9 T magnetic field and 5 V under zero field for sample p40–500 and 1 V under 9 T field and 10 V under zero field for sample p50–700.

Supporting Information

Supporting Information is available from the Wiley Online Library or from the author.

Acknowledgements

The authors acknowledge the Jenny and Antti Wihuri Foundation and the University of Turku Graduate School (UTUGS) for financial support. Sayani Majumdar acknowledges KONE foundation for financial support. The authors would like to thank T. Ahlqvist for help in sample preparation and Dr. T. Hynninen for assistance in illustration.

Received: June 2, 2015
Published online: July 14, 2015

[1] A. Chen, in *Emerging Nanoelectronic Devices*, (Eds: A. Chen, J. Hutchby, V. Zhirnov, G. Bourianoff), John Wiley & Sons Ltd, Chichester, UK **2015**, Ch. 9.
[2] A. Herpers, C. Lenser, C. Park, F. Offi, F. Borgatti, G. Panaccione, S. Menzel, R. Waser, R. Dittmann, *Adv. Mater.* **2014**, *26*, 2730.
[3] H. S. Lee, S. G. Choi, H.-H. Park, M. J. Rozenberg, *Sci. Rep.* **2013**, *3*, 1704.
[4] J. Lee, M. Jo, D. jun Seong, J. Shin, H. Hwang, *Microelectron. Eng.* **2011**, *88*, 1113.
[5] M. J. Rozenberg, M. J. Sánchez, R. Weht, C. Acha, F. Gomez-Marlasca, P. Levy, *Phys. Rev. B* **2010**, *81*, 115101.
[6] A. Sawa, *Mater. Today* **2008**, *11*, 28.
[7] H. Sun, Q. Liu, C. Li, S. Long, H. Lv, C. Bi, Z. Huo, L. Li, M. Liu, *Adv. Funct. Mater.* **2014**, *24*, 5679.
[8] A. Asamitsu, Y. Tomioka, H. Kuwahara, Y. Tokura, *Nature* **1997**, *388*, 50.
[9] Y. Tomioka, A. Asamitsu, H. Kuwahara, Y. Moritomo, Y. Tokura, *Phys. Rev. B* **1996**, *53*, R1689.
[10] T. Elovaara, H. Huhtinen, S. Majumdar, P. Paturi, *J. Phys.: Condens. Matter* **2012**, *24*, 216002.
[11] M. R. Lees, J. Barratt, G. Balakrishnan, D. M. Paul, C. D. Dewhurst, *J. Phys.: Condens. Matter* **1996**, *8*, 2967.
[12] T. Elovaara, T. Ahlqvist, S. Majumdar, H. Huhtinen, P. Paturi, *J. Magn. Magn. Mater.* **2015**, *381*, 194.
[13] K. Miyano, T. Tanaka, Y. Tomioka, Y. Tokura, *Phys. Rev. Lett.* **1997**, *78*, 4257.
[14] N. Takubo, Y. Ogimoto, M. Nakamura, H. Tamaru, M. Izumi, K. Miyano, *Phys. Rev. Lett.* **2005**, *95*, 017404.
[15] N. Takubo, I. Onishi, K. Takubo, T. Mizokawa, K. Miyano, *Phys. Rev. Lett.* **2008**, *101*, 177403.
[16] P. Beaud, A. Caviezel, S. O. Mariager, L. Rettig, G. Ingold, C. Dornes, S.-W. Huang, J. A. Johnson, M. Radovic, T. Huber, T. Kubacka, A. Ferrer, H. T. Lemke, M. Chollet, D. Zhu, J. M. Glownia, M. Sikorski, A. Robert, H. Wadati, M. Nakamura, M. Kawasaki, Y. Tokura, S. L. Johnson, U. Staub, *Nat. Mater.* **2014**, *13*, 923.
[17] S. Majumdar, H. Huhtinen, M. Svedberg, P. Paturi, S. Granroth, K. Kooser, *J. Phys.: Condens. Matter.* **2011**, *23*, 466002.
[18] S. M. Sze, *Semiconductor Devices, Physics and Technology*, Wiley, New York, NY, USA **1985**, p.43.
[19] M. Garganourakis, V. Scagnoli, S. W. Huang, U. Staub, H. Wadati, M. Nakamura, V. A. Guzenko, M. Kawasaki, Y. Tokura, *Phys. Rev. Lett.* **2012**, *109*, 157203.
[20] H. A. Jahn, E. Teller, *Proc. R. Soc. London A* **1937**, *161*, 220.
[21] E. E. Rodriguez, T. Proffen, A. Llobet, J. J. Rhyne, J. F. Mitchell, *Phys. Rev. B* **2005**, *71*, 104430.
[22] P. G. Radaelli, R. M. Ibberson, D. N. Argyriou, H. Casalta, K. H. Andersen, S.-W. Cheong, J. F. Mitchell, *Phys. Rev. B* **2001**, *63*, 172419.
[23] P. G. Radaelli, D. E. Cox, M. Marezio, S.-W. Sheong, *Phys. Rev. B* **1997**, *55*, 3015.
[24] A. Daoud-Aladine, J. Rodriguez-Carvajal, L. Pinsard-Gaudart, M. T. Fernandez-Diaz, A. Revcolevschi, *Phys. Rev. Lett.* **2002**, *89*, 097205.
[25] C. Jooss, R. Warthmann, A. Forkl, H. Kronmüller, *Physica C* **1998**, *199*, 215.
[26] D. V. Efremov, J. van der Brink, D. I. Khomskii, *Nat. Mater.* **2004**, *3*, 853.
[27] C. H. Patterson, *Phys. Rev. B* **2005**, *72*, 085125.
[28] S. Picozzi, C. Ederer, *J. Phys.: Condens. Matter.* **2009**, *21*, 303201.
[29] H. Wadati, J. Geck, E. Schierle, R. Sutarto, F. He, D. G. Hawthorn, M. Nakamura, M. Kawasaki, Y. Tokura, G. A. Sawatzky, *New J. Phys.* **2014**, *16*, 033006.
[30] A. J. Millis, in *Theory of CMR Manganites*, Vol. 2 (Ed: Y. Tokura), Gordon and Breach Science Publishers, Amsterdam, The Netherlands **2000** Ch. 2.
[31] Y. Tokura, Y. Tomioka, *J. Magn. Magn. Mater.* **1999**, *200*, 1.
[32] J. H. Jung, K. H. Kim, T. W. Noh, E. Choi, J. Yu, *Phys. Rev. B* **1997**, *57*, R11043.
[33] P. Beaud, S. L. Johnson, E. Vorobeva, U. Staub, R. A. D. Souza, C. J. Milne, Q. X. Jia, G. Ingold, *Phys. Rev. Lett.* **2009**, *103*, 155702.
[34] P. Polli, M. Rini, S. Wall, R. W. Schoenlein, Y. Tomioka, Y. Tokura, G. Cerullo, A. Cavalleri, *Nat. Mater.* **2007**, *6*, 643.
[35] S. Bhattacharya, S. Pal, A. Banerjee, H. D. Yang, B. K. Chaudhuri, *J. Chem. Phys.* **2003**, *119*, 3972.
[36] G.-M. Zhao, V. Smolyaninova, W. Prellier, H. Keller, *Phys. Rev. Lett.* **2000**, *84*, 6086.
[37] A. Dagotto, T. Hotta, A. Moreo, *Phys. Rep.* **2001**, *344*, 1.